Modeling the Color of Multi-Colored Halftones

J A Stephen Viggiano*

ABSTRACT

A mathematical model which provides the relationship between the dot areas of a combination of halftone patterns and the color produced by such multi-colored halftone patterns is disclosed. Such a model has application in calibration of digital color systems, digital picture exchange, and the simulation of "spot color" using process color techniques.

The new model is an extension of the Spectral Yule-Nielsen model described by this author at a previous TAGA conference. It provides greater accuracy than the Neugebauer model, either with or without the Yule-Nielsen correction.

Experimental verification of the Demichel dot overlap model is presented. The Demichel model was found to be accurate for halftone patterns superimposed at a 30 degree orientation.

The new model provides an acceptable level of accuracy for many applications. In an experimental evaluation, many predictions of the new model were sufficiently close to measured color so as to be indistinguishable to a human observer.

INTRODUCTION

In this paper, we shall examine a mathematical model for the color produced by a combination of colored halftone patterns. Such combinations are used extensively in printing and publishing; 4-Color Process printing (using Cyan, Magenta, Yellow, and Black, or "CMYK," inks) is perhaps the most popular example. The model will thus be examined primarily from a 4-Color Process point of view.

---

* RIT Research Corporation, Graphics Division

Motivation

This model has been used to calibrate Digital Color Prepress and Digital Color Proofing Systems. In such systems, it is necessary to have accurate knowledge of the relationship between each color ultimately printed and the CMYK halftone dot areas used to create each printed color.

This relationship is also important in the exchange of digital picture information. Because color separation files are highly condition-specific, it is imperative to know not only the conditions assumed for the ultimate printing of the picture files being exchanged, but exactly how the files need to be adjusted in order to compensate for differences in these conditions. This situation can arise even at a single site, without the need for actual transmission to a different site, such as when separation films need to be generated for both Offset Lithography and Gravure. [1]

How important is this link to digital image exchange? One article says, "The need for data on how an electronic image will appear in print is becoming critical . . . ." [2] Unfortunately, the models in the prior art are not accurate enough, because the writer continues: "Because no effective models exist to relate the combined effect of colored halftone dots on paper, the relationship between electronic image data (and / or dots on film) and the visual appearance of the printed image is undefined. . . . [T]he need for this data becomes critical." The model disclosed here is accurate enough to meet the needs of digital image exchange, as well as a variety of other applications.

This model also has application in package printing, where a number of uniformly colored areas often need to be produced. This situation is referred to as "spot" color, and is usually handled by printing each area separately, using a custom-mixed ink for each spot color. This is a practical solution if the number of spot colors is one or two, but becomes impractical when large numbers of spot colors are desired. If process and spot color are to appear on the same sheet, only two spot colors can be accommodated in a single run through a six-unit sheetfed press.

Pobboravsky and Pearson, in a 1972 TAGA Paper, describe a method for determining the halftone dot areas required to match a colorimetrically specified color, using the process inks. [3] The method they discussed was based on an older version of the model described in this paper. The basic techniques and principles are similar, however.

Greater accuracy may be obtained by replacing the model used in the 1972 paper with the model disclosed here.

Evolution of the Model

The evolution of this model has occurred over a period spanning more than half a century. Until the 1930s, there was no such model. In 1937, Neugebauer published his seminal paper, [4] which disclosed the equations which bear his name. Until 1951, the accuracy of the model was limited by the scattering of light within the paper, because the reflection did not occur at the ink-paper interface. (Indeed, it is generally conceded that when printing with normal inks on normal paper, there is no well-defined interface between the ink and paper.) The work of Yule and Nielsen, [5] and Yule and Colt, [6] helped remove this obstacle.

The effect of Dot Gain was not usually taken into consideration for another decade or so. Lack of knowledge of the correct value of Yule and Nielsen's parameter, n, to use under the variety of conditions which prevail limited both the accuracy and the acceptance of the model. Pearson published a paper in 1980 which demonstrated that a value of 1.7 is reasonable [7] in lack of more specific information. Until 1985, the Yule-Nielsen model was being applied to wideband measurements. This author demonstrated that the nature of the Yule-Nielsen model precludes the use of wideband measurements, and, in order to obtain the necessary level of accuracy, spectrophotometric measurements must be used. [8]

There are two additional factors which limit the accuracy of the new model. The most important is the non-uniformity of the microdensity of printed halftone dots. Rather than cylindrical, "hard" dots (to borrow a phrase from processwork), printed halftone dots tend to be mound shaped, "soft" dots — gradually increasing in density from their edges, to a maximum value near their core. Again, in the parlance of the processworker, printed halftone dots exhibit a "fringe."

This fringe can cause experimentally determined values of n to become large, exceeding the theoretical limit of 2. [9] This is the effect which contributed most to Pope's [10] observation of infinite n values (particularly in the secondary and tertiary absorption bands) in a recent investigation.

In addition, the assumption is made that there exists a well-defined interface between the ink and paper. With the exception of prepress proofing processes and printing on certain papers, this is not the case.

These two additional factors are beyond the scope of the present study; we plan to address them in the future.

Table 1 presents an approximate (by decade) timetable of these accuracy-limiting factors and when they were in effect. The last two factors share the dubious honor of being, in our opinion, the current accuracy-limiting factors.

Year	**Accuracy Limiting Factor**
1930	No Model
1950	Scattering of Light in Substrate
1960	Dot Gain
1970	Lack of Knowledge of n
1980	Wideband Measurements
1990	Nonuniformity of Dot Density
1990	Penetration of Ink in Paper

Table 1.
Factors Limiting the Accuracy of Dot Area / Color Models

THE NEUGEBAUER MODEL

In 1937, Hans Neugebauer published a model for the color of multi-colored overprinted halftone patterns. In its derivation, Neugebauer assumes an essentially additive color model. In the literature are excellent derivations of this model; here we shall be content with the explanation that, under Additive Color Theory, the reflectance of a print is simply the sum of the reflectance of each combination of ink, weighting each by the relative proportion of the paper that it occupies. Each ink combination, then, is a primary under this additive model; we may refer to these combinations as *Neugebauer Primaries*. In Figure 1, we illustrate, schematically with a Venn diagram, the partial overlap of three halftone dots — one Cyan, one Magenta, and the other Yellow — and the eight Neugebauer Primaries they produce, counting the unprinted area of the paper, as well.

The Neugebauer model may be expressed symbolically as:

$$(1) \qquad R = a_pR_p + a_cR_c + a_mR_m + a_yR_y + a_rR_r + a_gR_g + a_bR_b + a_3R_3$$

where R is the reflectance of the multicolored tint*, each R_i is the reflectance of the corresponding primary; each a_i is the relative areas of the paper covered by the indicated primary; and the subscripts $_{p, c, m, y, r, g, b,}$ and $_3$ denote the primary under consideration (Paper, Cyan, Magenta, Yellow, Red, Green, Blue, and 3-Color Overprint, respectively).

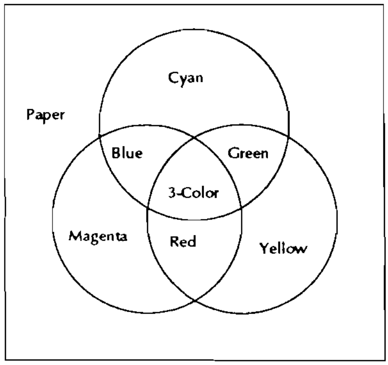

Figure 1.
Schematic illustration of the generation of eight Neugebauer Primaries from the overlap of Cyan, Magenta, and Yellow halftone dots.

Neugebauer went further, using a model by Demichel for the relative area of each primary. These relative areas relate to the halftone dot areas on paper of the Cyan, Magenta, and Yellow halftone dots, which we shall refer to as c, m, and y, respectively. These areas are:

$$
\begin{aligned}
a_p &= (1 - c)(1 - m)(1 - y) \\
a_c &= c(1 - m)(1 - y) \\
a_m &= m(1 - c)(1 - y) \\
a_y &= y(1 - c)(1 - m) \\
a_r &= m\,y(1 - c) \\
a_g &= c\,y(1 - m) \\
a_b &= c\,m(1 - y) \\
a_3 &= c\,m\,y
\end{aligned}
\tag{2}
$$

* Some authors use the symbol R for the red reflectance only, and G and B, respectively, for the green and blue reflectances. Here we use R to denote reflectance in general.

Note that each area contains the term (1 - c) if Cyan ink is not used to print that particular primary, or the term c if Cyan ink is included. An analogous observation holds for Magenta and Yellow. This may be justified intuitively: the area covered by a combination of several inks, if printed in a random arrangement, should equal the products of the proportion of paper covered by each of the inks individually. This may be termed a stochastic (or probabilistic) justification for the Demichel model of dot overlap.

Because of the stochastic appearance of this model, it has come under criticism as being perhaps too simplified. Halftone patterns are periodic, and might not exhibit the statistical independence necessary for the Demichel model to hold. Certainly, we would not expect this model to be valid for dot-on-dot printing.

The details of an experiment we performed to test the validity of the Demichel model are presented in the experimental section of this paper.

Extension to 4-Color Case:
With the addition of Black ink, we double the number of possible overlaps, so we have 16 primaries rather than just 8. The generalization to the four-color case is not complicated, and basically involves considering the original eight primaries both in their original state, and with the overprinting of black ink. The areas given in Equation Set (2) are repeated and modified, so that a total of 16 areas may be computed.

The Appendix contains the actual equations used in the 4-color case.

Accuracy of the Neugebauer Equations
Several investigations in the literature demonstrate the inaccuracy of the Neugebauer model. Pobboravsky, [11] for example, found that they were not accurate enough for determination of gray balance requirements, and resorted to empirical equations.

We often use the CIELAB color difference, ΔE^*, as a measure of how well the predictions of a mathematical color model fit actual measurements. In our experimental work, we have found that the Neugebauer model provides good results (arbitrarily, $\Delta E^* \leq 2$) in some portions of color space, fair predictions in other portions ($2 < \Delta E^* \leq 6$), and poor predictions ($\Delta E^* > 6$) in yet others. ΔE^* values as high as 30 have been observed; this is five times the figure suggested by Stamm as allowable for the total variation in the printing process. [12]

These large ΔE^* values tend to arise when one or more of the chromatic inks is printing as a midtone dot, *i.e.*, in the vicinity of 50 percent. The Neugebauer model is assured of matching any of the primary conditions (all dot areas either zero or one) as accurately as the measurements of the primaries we are using to make the predictions.

The Yule-Nielsen Modification:
Yule and Nielsen, in 1951, published a paper which considered the effect of the penetration of light into the paper, and demonstrated a significant increase in accuracy over a model which ignores this effect. [5] Their model was for a single-color halftone tint. Cast in terms of reflectances, the Yule-Nielsen model for a Cyan tint is:

$$(3) \qquad R = [(1 - c)\, R_p{}^u + c\, R_c{}^u]^n$$

where n is the Yule-Nielsen parameter; and u is 1/n, a subtle visual pun. The other symbols are as previously defined. Note that we may re-write Equation (3) as:

$$(3a) \qquad R^u = (1 - c)\, R_p{}^u + c\, R_c{}^u$$

or

$$(3b) \qquad R' = (1 - c)\, R_p' + c\, R_c'$$

where $R' = R^u$ and $R_c' = R_c{}^u$. The Yule-Nielsen n-value depends upon several factors; the screen frequency and type of paper are perhaps the most important two.

Note that Equation (3b) resembles the Neugebauer model. With the exception of the primed reflectances, Equation (3b) is a special case of Equation (1); the two are equal when m = y = 0. This relationship suggests the Yule-Nielsen modified Neugebauer equation, which is:

$$(1a) \qquad R' = a_p R'_p + a_c R'_c + a_m R'_m + a_y R'_y + a_r R'_r + a_g R'_g + a_b R'_b + a_3 R'_3$$

The area of each primary is computed as before, using Equation Set (2).

This model, called the Yule-Nielsen Modified Neugebauer Model, was first suggested by Yule and Colt [6] in 1951, and elucidated by Yule (in a paper by Pearson) in 1964. [13] Again, the generalization to the four-color case is presented in the Appendix.

Accuracy of the Yule-Nielsen Modified Neugebauer Model
In his 1966 gray balance investigation, Pobboravsky tried the modified Neugebauer model. Pobboravsky's conclusion was ". . . that the modified equations produced no significant increase in agreement over the unmodified equations."

A NEW MODEL

In a 1985 TAGA paper, this author investigated the use of the Yule Nielsen model to predict the color of single-colored halftone tints, and concluded that the non-linearities in (3) require that narrowband measurements be used. [8] This is because the non-linearities in Equation (3) require that the reflectance curve of each primary be nearly constant in each prediction band.

Perhaps the only way to insure that this condition is in general fulfilled is to use very narrow bands. The bandwidth of each Status T densitometer channel is approximately 70 nm; the reflectance spectra of the primaries (except for the Black ink, and perhaps the paper) will vary considerably over such a range. Spectrophotometric measurements, with bandwidths of 10nm or smaller, were able to provide a significant increase in the accuracy of the color predicted for single-color halftone tints.

If we use the symbol R_λ to denote the reflectance of the tint at wavelength λ, and the reflectances of the primaries in an analogous manner, we may consider the following model for the spectral reflectance of 3-color halftone tints:

$$(4) \qquad R'_\lambda = a_p R'_{\lambda p} + a_c R'_{\lambda c} + a_m R'_{\lambda m} + a_y R'_{\lambda y} + a_r R'_{\lambda r} + a_g R'_{\lambda g} + a_b R'_{\lambda b} + a_3 R'_{\lambda 3}$$

Equation (4) may be applied for each wavelength in a sampled spectrum, so that a sampled spectrum for the tint may be predicted. (Note that it is necessary to raise R'_λ to the power of n to obtain the spectral reflectance.)

This reflectance spectrum may then be integrated to yield Tristimulus Values or Status T reflectances, which can be converted into densities.

In this investigation, we shall compute tristimulus values, which shall be converted into CIELAB coordinates.

As for the other models, the technique for generalizing to the 4-color case is presented in the Appendix.

Compensation for Dot Gain
As halftone images make their way from film, to plate, to press, they tend to change in size. If not compensated for, this effect, referred to as Dot Gain, can cause inaccuracies in the predictions of a model.

Implied in the derivation of Equations (1), (1a), (3) and (4) is that the a values will be calculated using the halftone dot areas on the paper, not on the film. If we know a halftone dot area on film, and would like to determine the corresponding halftone dot area on the paper, we may use an equation such as: [14]

$$(5) \qquad a_p = a_f + 2\,\Delta_p\,[a_f\,(1 - a_f)]^{1/2}$$

where a_p is the dot area on paper; a_f is the dot area on film, and Δ_p is the amount of dot gain when $a_f = 0.50$ (50 percent). It is still necessary to determine the dot gain for at least one point, but the relationship between the dot areas on film and paper is a fundamental one.

Conversion of Digital Halftone Value into Dot Area
This step is highly site- and condition dependent. In our case, we found it sufficient to divide the digital halftone value by 255, which represented the fully-inked condition, and use a transfer of the type given by Equation (5) to yield dot area on film. Because we will require an additional transfer to represent the step from film to paper, we cascaded two curves together, as described in the literature. [14] For the transfer from digital halftone value to dot area on film, we used the parameter Δ_d. The parameter Δ_p retained its original interpretation as the dot gain at 50 percent in the film to paper transfer.

EXPERIMENTAL

Verification of the Demichel Model of Dot Overlap
We conducted an experiment to determine if the Demichel model is valid for halftone patterns oriented 30 degrees from each other, which exhibit a tight moiré pattern. Because of the difficulty with which the relative area of halftone patterns printed on paper may be measured, we chose to use hard-dot halftone tint screens, which may be easily

measured in transmission. Because we are interested here in testing the area of overlap of two halftone tint patterns, there should be no loss of validity to substitute tints on film for tints on paper; the fundamental geometric properties remain unchanged.

It should suffice to examine pairs of overlaid tint screens. If any deviation from Demichel's predicted performance would be observable using three tints, it should be also present when using two. If the tint screens are measured as halftone positives, the area of the combination, under Demichel's model, may be expressed as:

$$(6) \qquad a_{1+2} = a_1 + a_2 - a_1 a_2$$

where a_1 and a_2 are the dot areas of the tints, individually, and a_{1+2} is the area of the two tints, overlapped.

These predicted values may be compared with the values actually measured. Because the halftone dot meter used in this experiment (a Tobias PCT) has a resolution of one percent halftone dot area, absolute, absolute deviations as large as two percent may exist, and deviations averaging slightly less than one percent could be expected. If the two sets of dot areas (*i.e.*, measured and predicted) differ by significantly more than one percent, we may conclude that the Demichel model for halftone dot overlap is inadequate.

Six tint screens, manufactured by the Beta Screen Corporation, were used. The dot areas ranged from approximately 25 to 80 percent, and the screen frequency was approximately 52 lines per centimeter (133 lines per inch). A small section of a light table, approximately one centimeter square, was masked off with stripping tape, and the area was checked for an even wash pattern (evenness of illumination). The selected portion of the table was found to have no more than one percent variation in illumination.

The dot area meter was then nulled so that a clear piece of tint screen gave a measurement of zero, and a solid area read 100 percent. Each tint screen was then measured four times, in a randomized order. These measurements appear in Table 2.

These dot areas varied by no more than one percent in each case; this indicates the evenness of the tint screens as well as the repeatability of the measurements. The PCT dot area meter was then nulled on two layers of film base prior to measuring the tint screens in combination.

The tint screens were then overlaid permutationally, emulsion facing emulsion so that any problems of parallax, etc., may be avoided. The dot areas of these overlaid tint screen pairs were then measured. The average values of each tint, from Table 2, were used to compute a predicted value for each combination of tint screens, in accordance with the Demichel model. Both the measured and predicted values appear in Table 3.

	Tint Screen Number					
	#1	#2	#3	#4	#5	#6
	0.25	0.36	0.55	0.64	0.71	0.80
	0.25	0.36	0.55	0.63	0.71	0.80
	0.25	0.36	0.55	0.64	0.71	0.80
	0.26	0.36	0.56	0.64	0.71	0.80
Averages:	0.253	0.360	0.553	0.638	0.710	0.800

Table 2.
Dot Areas of Hard Dot Tints.

	Halftone Dot Areas		
Tint Pair	Obs. 1	Obs. 2	Predicted
1 & 2	0.52	0.52	0.522
1 & 3	0.66	0.66	0.666
1 & 4	0.72	0.73	0.730
1 & 5	0.78	0.79	0.783
1 & 6	0.85	0.85	0.851
2 & 3	0.71	0.71	0.714
2 & 4	0.76	0.77	0.768
2 & 5	0.81	0.82	0.814
2 & 6	0.87	0.87	0.872
3 & 4	0.83	0.84	0.838
3 & 5	0.87	0.87	0.870
3 & 6	0.91	0.91	0.911
4 & 5	0.89	0.90	0.895
4 & 6	0.93	0.93	0.928
5 & 6	0.94	0.94	0.942

Table 3.
Observed and Predicted Dot Areas of Tint Pairs.

The largest deviation between a value predicted using the Demichel model of dot overlap and the measurement of the corresponding tint combination is one percent dot area. This is well within our pre-established tolerance, and we may conclude that the Demichel model for halftone dot overlap is accurate. It could also be inferred that any inadequacies in the accuracy of the Neugebauer model arise from failure of the other premise used in its derivation, viz, that the reflectance of a multicolored halftone tint exhibits linear additive behavior.

Verification of the New Model

A special test object was prepared for the evaluation of the accuracy of the new model. This test object was generated digitally, and transmitted to a Scitex system for output. Films were generated, and from these films were made Signature* proofs. An additional target was included so that the translation from digital halftone value and dot area on paper could be determined. This additional target also contained all 16 of the Neugebauer Primaries for 4-color printing.

The test target was composed of 25 separate halftone patches of different colors. The composition of this target is given in Table 4. Each patch is identified by its row and column number. The digital halftone values, on a scale from zero (uninked) to 255 (fully inked) are given.

	DIGITAL HALFTONE VALUE			
Patch	C	M	Y	K
1, 1	28	121	0	0
1, 2	121	0	176	0
1, 3	176	28	71	0
1, 4	0	71	28	0
1, 5	28	121	71	28
2, 1	121	28	121	28
2, 2	0	176	71	0
2, 3	71	121	28	0

Table 4 (Part 1).
Composition of the Test Target.

* Signature is a trademark of the Eastman Kodak Company.

2, 4	28	0	121	0
2, 5	121	28	0	0
3, 1	71	0	71	0
3, 2	28	28	28	0
3, 3	71	28	71	28
3, 4	176	176	0	0
3, 5	0	121	176	0
4, 1	121	176	28	0
4, 2	71	28	28	71
4, 3	28	176	121	121
4, 4	71	28	176	0
4, 5	28	71	71	0
5, 1	0	28	212	0
5, 2	71	71	0	0
5, 3	28	176	176	0
5, 4	71	71	28	28
5, 5	176	0	28	0

Table 4 (Part 2).
Composition of the Test Target.

The transfer from digital halftone value to dot area on paper is characterized by two parameters for each channel. The values of these parameters used in this investigation appear in Table 5. These values are highly condition and site dependent, and vary from installation to installation, as well as from day to day. A Yule-Nielsen n value of 2.00 had been determined to be optimum for our conditions, which included a 150 line per inch halftone frequency, and a coated stock.

Separation	Δ_d	Δ_p
Cyan	0.0907	-0.1172
Magenta	0.0739	-0.1039
Yellow	0.0937	-0.1144
Black	0.0947	-0.1382

Table 5.
Dot Gain Parameters.

Knowing this information, it is possible to determine the halftone dot areas on paper for each patch. Because this target is used only for testing purposes, discrete digital halftone values were selected to make this translation simple. Table 6 lists all the halftone dot areas on paper which correspond to values used in the test target.

Digital Value	Separation Cyan	Magenta	Yellow	Black
0	0.0000	0.0000	0.0000	0.0000
28	0.0792	0.0806	0.0828	0.0654
71	0.2472	0.2459	0.2524	0.2304
121	0.4489	0.4449	0.4548	0.4322
176	0.6761	0.6696	0.6816	0.6629

Table 6.
Digital Value to Dot Area on Paper Translation.

The values in Table 6 were simply substituted into Equation Set (A2), which is the four-color version of Equation Set (2), and these values, together with the reflectance spectra of the 16 Neugebauer Primaries, were used in Equation (A4) in order to make predictions of the spectrum of each patch in the test target. These predictions were then compared to measurements of the actual patches, and the total color difference, ΔE^*, was computed. These comparisons appear in Table 7.

DISCUSSION

Because of the skewed nature of ΔE^* values, it is more appropriate to use their geometric mean (average), rather then their arithmetic mean. (The distribution of the logarithms of ΔE^* values tends to be roughly gaussian.) The geometric mean of the ΔE^* values in Table 7 is 1.82; this indicates that the new model provides excellent predictions of the color of each of these patches. It is worth mentioning that the test image was used for verification purposes; the model was calibrated using the other target.

Another measure of the goodness of the predictions is given by the largest value of ΔE^*. This is 3.70, which, while not perfect, is a desirable cap for all the values.

	Measured			Predicted			
Patch	L*	a*	b*	L*	a*	b*	ΔE*
1, 1	69.56	27.06	-4.29	70.85	28.83	-4.37	2.20
1, 2	73.36	-23.92	32.96	74.54	-24.34	30.30	2.94
1, 3	62.44	-24.04	-15.39	64.55	-24.67	-15.08	2.22
1, 4	81.89	15.70	6.42	82.42	16.21	6.34	0.74
1, 5	65.05	23.29	8.51	67.22	25.72	10.27	3.70
2, 1	67.99	-14.79	10.13	69.15	-16.30	10.86	2.04
2, 2	60.76	49.33	13.05	62.56	48.23	11.57	2.57
2, 3	64.64	20.08	-7.05	65.18	21.35	-7.20	1.39
2, 4	88.50	-7.56	32.46	89.55	-6.58	34.26	2.31
2, 5	72.94	-8.86	-20.16	73.98	-10.20	-19.74	1.75
3, 1	83.68	-10.86	9.07	83.86	-11.05	9.15	0.27
3, 2	85.81	2.02	2.78	87.20	2.12	4.56	2.26
3, 3	75.05	-4.81	6.65	77.07	-5.72	7.60	2.40
3, 4	41.19	18.81	-29.26	42.46	19.55	-30.89	2.19
3, 5	71.45	26.77	43.51	71.73	27.92	42.81	1.38
4, 1	49.26	30.04	-14.76	49.22	29.64	-17.09	2.37
4, 2	68.95	-2.87	-4.80	68.83	-3.33	-3.29	1.58
4, 3	41.46	30.23	11.29	42.10	31.51	13.04	2.26
4, 4	77.59	-8.60	39.97	79.03	-9.60	40.43	2.04
4, 5	78.44	10.02	12.39	79.18	11.82	13.93	2.48
5, 1	88.27	2.93	35.18	88.90	1.72	36.65	2.01
5, 2	73.92	7.37	-10.02	74.18	8.07	-10.81	1.08
5, 3	57.18	42.45	31.82	59.35	43.07	32.22	2.29
5, 4	69.52	5.49	-5.85	69.96	6.68	-5.28	1.40
5, 5	67.07	-25.29	-27.38	68.34	-25.62	-25.63	2.19

Table 7.
Comparison of Measured and Predicted Colors.

CONCLUSIONS

A new model for the prediction of color of multi-colored halftones was presented. It is a generalization of the Neugebauer model, using the Spectral Yule-Nielsen modification. Spectrophotometric measurements of the Neugebauer primaries, together with dot gain information, are used to effect predictions of a printed area's reflectance spectrum. This spectrum can be used to compute Status T densities, Tristimulus Values, CIELAB Color Coordinates, etc.

The predictions made by the new model are sufficiently accurate for many purposes, particularly those mentioned in the Introduction. It may be concluded that the difficulties experienced in the past when using models of the Neugebauer type were a result of the penetration of light into the paper (Yule-Nielsen effect) and failure of the Yule-Nielsen model to perform well when applied to wideband measurements.

The necessity of measuring all possible combinations of overprints is awkward and time consuming. It is desirable to have a model which requires spectra of only the individual inks, and obtains the spectra of the overprints through a separate model. This is being addressed.

ACKNOWLEDGMENTS

Part of this research was performed under contract to the Graphic Imaging Systems Division of the Eastman Kodak Company. The author thanks GISD for their kind permission to use this material.

Part of this investigation served as a portion of the author's Master's Thesis at RIT's School of Printing Management and Sciences. The author wishes to extend his thanks to the Navigators, a New-York based Graphic Arts society, for providing financial assistance during his graduate studies.

Mr Philip Tobias of Tobias Associates generously loaned the author a PCT halftone dot area meter during his thesis investigation.

This paper is dedicated to Dr John A C Yule.

APPENDIX

Generalization of the Model to the Four-Color Case

The equations in this appendix will start with an A; the number of the corresponding equation from the text will follow.

The halftone dot areas are computed using the formulas:

$$
\begin{aligned}
a_p &= (1 - c)(1 - m)(1 - y)(1 - k) \\
a_c &= c(1 - m)(1 - y)(1 - k) \\
a_m &= m(1 - c)(1 - y)(1 - k) \\
a_y &= y(1 - c)(1 - m)(1 - k) \\
a_r &= m\,y(1 - c)(1 - k) \\
a_g &= c\,y(1 - m)(1 - k) \\
a_b &= c\,m(1 - y)(1 - k) \\
a_3 &= c\,m\,y(1 - k) \\
a_k &= k(1 - c)(1 - m)(1 - y) \\
a_{ck} &= c\,k(1 - m)(1 - y) \\
a_{mk} &= m\,k(1 - c)(1 - y) \\
a_{yk} &= y\,k(1 - c)(1 - m) \\
a_{rk} &= m\,y\,k(1 - c) \\
a_{gk} &= c\,y\,k(1 - m) \\
a_{bk} &= c\,m\,k(1 - y) \\
a_4 &= c\,m\,y\,k
\end{aligned}
\tag{A2}
$$

where k is the halftone dot area on paper of the black; the subscript $_4$ indicates the 4-color overprint, and the subscripts $_{ck,\ mk,\ yk,\ rk,}$ etc. refer to the combinations cyan and black, magenta and black, and so on.

Note that the first eight equations are the same as in Equation Set (2), aside from the additional factor of (1 - k). Similarly, the last eight equations are similar to those in Equation Set (2), but with slightly different names, and with the factor k multiplied in. This observation should guide the reader if generalization to even larger numbers of colors is desired.

The reflectance of a 4-color halftone pattern, under Neugebauer's model, is:

$$
\begin{aligned}
R = {} & a_pR_p + a_cR_c + a_mR_m + a_yR_y + a_rR_r + a_gR_g + a_bR_b + a_3R_3 \\
& + a_kR_k + a_{ck}R_{ck} + a_{mk}R_{mk} + a_{yk}R_{yk} + a_{rk}R_{rk} + a_{gk}R_{gk} \\
& + a_{bk}R_{bk} + a_4R_4
\end{aligned}
\tag{A1}
$$

The equation corresponding to Equation (1a), which would provide the reflectance of a four-color halftone using the Yule-Nielsen modification, may be obtained by replacing all Rs in Equation (A1) with their primed counterparts.
Using the new model, it is:

$$(A4) \qquad R'_\lambda = a_p R'_{\lambda p} + a_c R'_{\lambda c} + a_m R'_{\lambda m} + a_y R'_{\lambda y} + a_r R'_{\lambda r} + a_g R'_{\lambda g} + a_b R'_{\lambda b} + a_3 R'_{\lambda 3} + a_k R'_{\lambda k} + a_{ck} R'_{\lambda ck} + a_{mk} R'_{\lambda mk} + a_{yk} R'_{\lambda yk} + a_{rk} R'_{\lambda rk} + a_{gk} R'_{\lambda gk} + a_{bk} R'_{\lambda bk} + a_4 R'_{\lambda 4}$$

LITERATURE CITED

1. Kaliser, Dennis, Multi process output from a common data base. *1984 TAGA Proceedings*, p 93 - 106.

2. Color Calibration and Communication for EIP [Electronically Integrated Publishing]. *The Dunn Report*, February, 1990.

3. Pobboravsky, Irving, and Milton Pearson, Computation of dot areas required to match a colorimetrically specified color using the modified Neugebauer equations. *1972 TAGA Proceedings*, p 65 - 77.

4. Neugebauer, H E J, Die theoretischen grundlagen des mehrfarbendruckes. *Zeitschrift Wissenschaften Photography*, 1937. 36 : 73 - 89.

5. Yule, J A C, and W J Neilsen, *[sic]* The penetration of light into paper and its effect on halftone reproduction. *1951 TAGA Proceedings*, p 65 - 76.

6. Yule, J A C, and R Colt, Colorimetric investigations in multicolor printing. *1951 TAGA Proceedings*, p 78.

7. Pearson, Milton, n value for general conditions. *1980 TAGA Proceedings*. p 415 - 425.

8. Viggiano, J A Stephen, The color of halftone tints. *1985 TAGA Proceedings*, p 647 - 661.

9. Ruckdeschel, F R, and O G Hauser, Yule-Nielsen effect in printing: a physical analysis. *Applied Optics*, 1978. 17 : 21, p 3376 - 83.

10. Pope, William W, A practical approach to n-value. *1989 TAGA Proceedings*, p 142 - 151.

11. Pobboravsky, Irving, Methods of computing ink amounts to produce a scale of neutrals for photomechanical reproduction. *1966 TAGA Proceedings*, p 10 - 34.

12. Stamm, Scott, An investigation of color tolerance. *1981 TAGA Proceedings*, p 156 - 173.

13. Pearson, Milton, The use of color gamut of an ink set in the selection of process inks, *1964 TAGA Proceedings*, p 59 - 74.

14. Viggiano, J A Stephen, The GRL dot gain model. *1983 TAGA Proceedings*, p 423 - 439.